ChemPubSoc Europe

DOI: 10.1002/slct.201904099

Chemistry SELECT Full Papers

Catalysis

$NaAlO_2$-Promoted Mesoporous Catalysts for Room temperature Knoevenagel Condensation Reaction

Sreerangappa Ramesh,* François Devred, and Damien P. Debecker[a]

Mesoporous solid base catalysts are essential candidates for green and sustainable catalytic processes. In this work, novel mesoporous solid base catalysts was synthesized by promoting mesoporous supports with sodium aluminate ($NaAlO_2$). The prepared catalysts are characterized using a wide variety of molecular and solid-state techniques to determine their structural and textural properties. The catalysts texture was strongly affected by the promotion of sodium aluminate. The nature of the support and the sodium aluminate loading are shown to play a crucial role on the total basicity. In turn, these $NaAlO_2$-containing mesoporous materials showed high catalytic activity for Knoevenagel condensation under solvent free reaction conditions. The catalysts are truly heterogeneous without leaching any active sites and also showed good reusability.

1. Introduction

In the context of sustainable chemistry, increasing attention has been given to the substitution of conventional homogeneous base catalysts (KOH, NaOH and alkali carbonates) with heterogeneous ones.[1–3] Solid catalysts allow easy separation from the reaction mixture, recovery of products, and subsequently make it facile to recycle the catalysts.[4,5] Hence, there is a need for the development of solid base catalysts and they are desirable for industrial production of chemicals, environmental friendly by providing the ease of separation and reuse.[6–8] The solid samples, act as catalysts either by abstraction of a proton from the reactants usually represented as Brønsted baseor contribution of an electron pair to the reactants from the catalyst to form anionic intermediates - Lewis base.[7] Numerous solid materials, which acts as effective base catalysts for various organic transformations are reported.[1]

Among heterogeneous base catalysts, mesoporous solid bases find interesting applications in environmentally friendly catalytic processes.[2,9] It was proved earlier that, the high surface areas and the abundant porous channels of these materials are beneficial for the diffusion of reactants.[2,10,11] They are particularly helpful with reactions involving bulky molecules due to the presence of the mesoporous structures, which largely expands the scope of the catalysis for valorization of various biomolecules .[9,12] Therefore, great efforts have been dedicated to fabricate mesoporous materials with tangible basicity.

Mesoporous materials possessing weak acidic or basic sites are not apposite candidates for catalytic applications.[9,10] In order to improve their catalytic performance, active species are incorporated into the pores and it can be done by various ways, such as impregnation, ion exchange, chemical vapor deposition, sol-gel processing and in-situ impregnation.[2,13] Among these methods, the introduction of active species into the mesoporous framework by impregnation method makes it possible to form uniform base sites distribution.[14] Such composite materials are therefore attracting attention for application as effective heterogeneous solid base catalysts for various organic transformations. Much attention has been given to generate basic sites on mesoporous supports by various methods[15,16] Amino group functionalized silica,[17] alkali metal doped carbon,[18] MnO_2 doped hexagonal mesoporous silica have been reported as solid mesoporous base catalysts recently.[10] Hence, mesoporous solid super base catalysts by one-pot synthesis with tunable basicity is having importance for selective organic transformations.

Sodium aluminate (SA), a solid super base catalyst, cheap and easily available material finds interesting applications in organic transformations[19–26] however, it is highly hygroscopic and corrosive, making its handling problematic. Blending, supporting or dispersing this highly reactive component would be a relevant strategy to optimize both catalytic activity and workability.[27,28] Previously, we incorporated SA on basic mixed oxides hydrotalcites by simple impregnation method.[28] The resulting materials possess strong basic site but textural properties were strongly affected (specific surface area and pore volume decreased by 20 folds).[28] Similar results are reported with sodium aluminate supported on different supports like Dolomite,[29] alumina[30] and titania.[31]

In the present study, we developed a strategy to incorporate sodium aluminate into mesoporous materials by one pot synthesis. Strong basicity can thus be generated by taking advantage of sodium aluminate and higher surface characteristics with mesoporous materials. As a result, a new type of

[a] Dr. S. Ramesh, Dr. F. Devred, Prof. D. P. Debecker
Institute of Condensed Matter and Nanosciences (IMCN),
UCLouvain, Place Louis Pasteur, 1, box L4.01.09, 1348 Louvain la-Neuve, Belgium
E-mail: kistramesh@gmail.com

Supporting information for this article is available on the WWW under https://doi.org/10.1002/slct.201904099

material featuring both mesoporosity and strong basicity was successfully fabricated. The new mesoporous solids are characterized in terms of texture, structure and basic properties. The catalytic performance of these new materials was probed in the Knoevegel condensation reaction (condensation of benzaldehyde with ethyl cyanoactate to produce ethyl-2-cyano-3-phenyl acryl ate) at room temperature without using any solvent.

2. Results and Discussion

The texture of the prepared mesoporous solids after calcination at 600 °C was first characterized by N_2 physisorption (Figure 1). The isotherms of all the prepared solid catalysts showed Type IV isotherms according to the IUPAC classification.[10] Meso porosity of the catalysts are confirmed from their relative pressure (p/p_0 = 0.6–0.75) (Figure S1). The extended hysteresis loop to a relative pressure of $p/p_0 \geqslant 0.90$, established the presence of textural inter-particle meso porosity.[32] The BET surface area (S_{BET}), average pore volume (V_p), average pore diameter calculated by the Barrett-Joyner-Halenda (BJH) method, and are listed in Table1. Mesoporous silica (M SiO_2) in its pure form showed high surface area of 470 m^2/ g, whereas after incorporation of sodium aluminate the specific surface area gradually decreases with increase in $NaAlO_2$ loading. However, it is interesting that, one-pot incorporation also decreases the surface area, which is much less when compared to catalysts prepared by impregnation method reported earlier.[28] The catalyst promoted with 20% $NaAlO_2$ showed 80–90 m^2/g, which is much higher when compared to pure sodium aluminate (2 m^2/g).

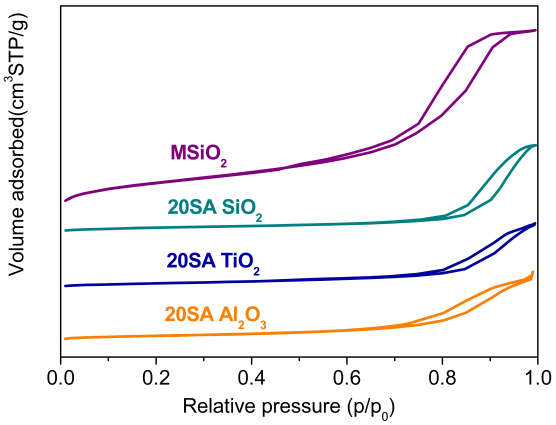

Figure 1. Nitrogen adsorption and desorption isotherms of catalysts.

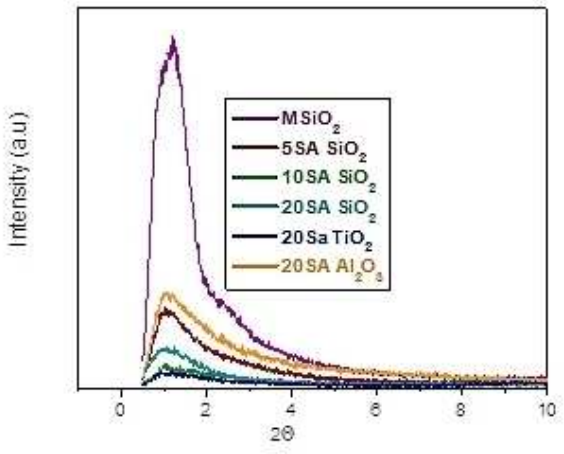

Figure 2. Powder XRD patterns of catalysts.

Figure 2 shows the low-angle XRD patterns of sodium aluminate promoted mesoporous materials of silica, alumina and titania after calcination at 600 °C. After $NaAlO_2$ promotion, the intensity of the peak reduced (20 SA SiO_2). These results imply disruption of the mesoporous structure and reduction of pore size and 20% sodium aluminate incorporated titania and alumina also showed the similar pattern. Figure S2, Supporting Information, displays the wide-angle XRD patterns of the mesoporous samples after calcination. Pristine silica sample present a broad signal centered at about 23°, which can be ascribed to amorphous silica walls.[10] Similar peak was observed after 5 and 10% SA incorporation, whereas with 20% SA resulted with decrease in peak intensity. Additionally, no additional peaks are observed on the samples even after 20% sodium aluminate promotion. This clearly demonstrated that, active species are well dispersed in the silica materials or that the particles of sodium aluminate species are smaller than the detection limit (~5 nm). Three peaks around $2\theta = 25.4$, 48, and 55° were observed for 20 SATiO_2, which are characteristic of anatase-type titania.[33,34] The intensity of XRD peaks of the sample reflects that the formed nanoparticles are crystalline and broad diffraction peaks indicate very small size crystallite. For the 20% SA incorporated in mesoporous alumina also showed the characteristic peaks for alumina at $2\theta = 47$ and 67° only.[35] Again, no diffraction peak assigned to crystalline $NaAlO_2$ was observed, suggesting that $NaAlO_2$ particles were well distributed in the materials and excluding the formation of larger crystals.

Using the temperature programmed desorption of carbon dioxide (CO_2-TPD), we have investigated the basicity of the prepared mesoporous solid catalysts and are represented in Figure 3. The quantity of desorbed CO_2 and the temperature of maximum desorption are the criteria for the total basic sites and basic strength respectively.[36,37] CO_2-TPD of pure silica did show any CO_2 desorption peak in the studied temperature range, confirming that it has no basic sites.[38] However, a drastic increase in total basicity is observed upon addition of $NaAlO_2$ on silica and it increases with increase in sodium aluminate loading (Table 1). Two distinct desorption peaks are observed for the 20 SASiO_2, one small peak around 200 °C and an intense peak at 700°C. The peak at lower temperature accounts for the weak basic sites, whereas, peak at higher temperature (700 °C) indicates the presence of strong basic site. Promotion of $NaAlO_2$ to titania and alumina showed both weak

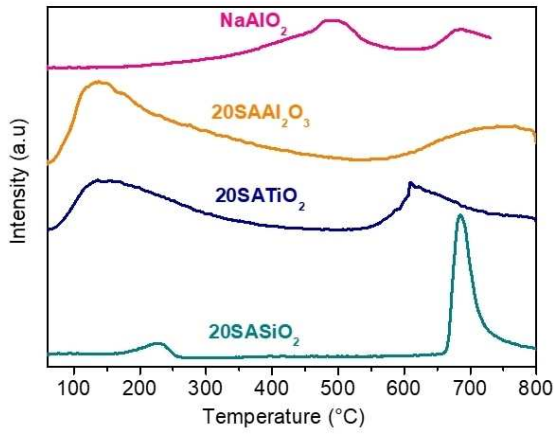

Figure 3. CO_2-TPD of the SA promoted mesoporous catalysts.

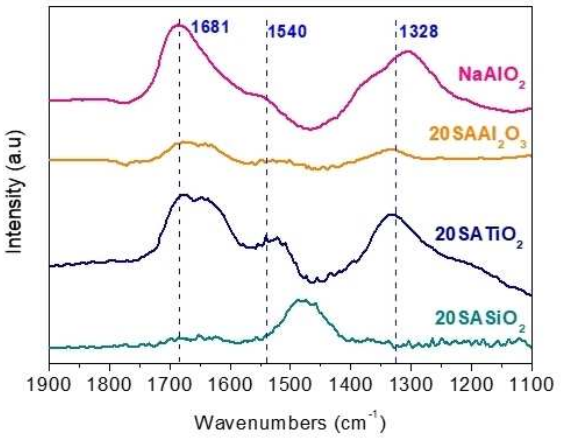

Figure 4. CO_2 DRIFT spectra of the SA promoted mesoporous catalysts.

Table 1. Physical properties of the catalysts.

Catalyst	Surface area (m^2/g)	Pore volume (cm^3/g)	Pore diameter (nm)	Amount of CO_2 desorbed/g of catalyst
$NaAlO_2$	2	0.1	21	0.47
20 SA Al_2O_3	90	0.4	12	0.064
SiO_2	470	1.0	8	–
5 SA-SiO_2	180	1.0	18	0.011
10 SA-SiO_2	100	0.6	18	0.019
20 SA SiO_2	90	0.5	17	0.030
20 SA TiO_2	90	0.4	14	0.036

and strong basic sites and in much higher quantity when compared to silica support. Pristine titania is slightly basic and it can absorb CO_2; upon incorporation of $NaAlO_2$ the catalyst displays both weak and strong basic sites in much higher concentration. Alumina being amphoteric material, after promotion of $NaAlO_2$, showed both weak and strong basic sites, the basicity of the catalysts are in the following order 20 $SASiO_2 < 20$ $SATiO_2 < 20$ $SAAl_2O_3$. Sodium aluminate belongs to a class of super base, possessing strong basic sites in much higher quantity compared to the SA promoted mesoporous materials.

To understand the different types of basic sites present in the prepared catalysts, further analysis was carried out by CO_2 adsorption with DRIFTS (Figure 4). CO_2 can interact with the catalyst in different modes to form different species (monodentate, bridged bidentate and chelating bidentate carbonate species), which indicates the presence of different types of surface basic sites.[39,40] It was reported earlier that, CO_2 adsorbed on oxygen ions with the lowest coordination number (monodentate) leads to strong basic sites and bridged bidentate carbonate and chelating bidentate carbonate adsorption can be assigned to moderate or weak basic sites.[39,40] Sodium aluminate showed three distinct peaks at 1681, 1540 and 1328 cm^{-1}corresponding three different mode of interaction of CO_2 with sodium aluminate.[26] The oxygen atom of $NaAlO_2$ can coordinate with CO_2 by monodentate modes - which leads to strong basicity (peak at 1328 cm^{-1}). The other two peaks at higher wave numbers corresponding to bridged and chelating mode of coordination, which leads to weak basicity (peaks at 1681 and 1540 cm^{-1}). However, 20 $SASiO_2$ showed two peaks- one at 1480 cm^{-1} that accounts for the monodentate coordination with the oxygen atom -possess strong basic sites, and a small peak around 1700 cm^{-1} which accounts for weak basic sites- also confirmed from CO_2-TPD. However, SA promoted titania and alumina samples resulted with all the three modes of bonding and possess strong and weak basic sites and it is also well correlated with CO_2-TPD results.

The prepared catalysts was tested in the Knoevenagel condensation of benzaldehyde (BA) with ethyl cyanoacetate (ECA) under solvent free reaction conditions (Scheme 1). Condensation reactions are very important in synthetic organic chemistry, which finds potential applications in the syntheses intermediates for anti-hypertensive drugs, pharmaceutical chemicals and natural products from small molecules.[41–43] The reaction is usually considered as a probe reaction for evaluating basic strength of the catalysts.[44–46] The target product, ethyl-2-cyano-3-phenyl acrylate, detected exclusively with all the

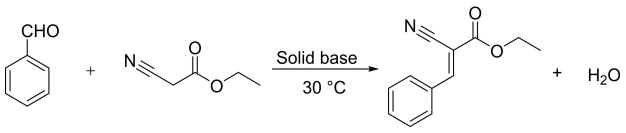

Scheme 1. Knoevenagel condensation of benzaldehyde with ethyl cyanoacetate.

catalysts studied for the screenings verified by GC and ^{1}H-NMR analysis (Figure S3).

In the absence of any catalyst, only a negligible BA conversion was observed, even after 4 h (BA conversion ~4%, see Table 2). In this case, the major product is benzoic acid-the oxidized product of benzaldehyde-as confirmed from GC analysis. Expectedly, the pristine mesoporous silica also showed very low activity (BA conversion of only 8% after 4 h of reaction time at 30 °C). The traditional solid base catalysts such as MgO and hydrotalcites calcined at 600 °C are also studied as benchmarks.

Mixed oxides derived from hydrotalcites possess strong and weak basic sites are active for the reaction studied (15% BA conversion). MgO showed moderate activity (54% BA conversion). On the other hand, the pure $NaAlO_2$ showed much higher activity in short reaction time, (~95% BA conversion in 2 h)actually, 58% BA conversion reached within 30 min of reaction.

In the condensation reaction of BA with ECA, the main function of the solid base catalyst is to support the abstraction of H^+ from active methylene compound (ECA), which will further react with the aldehyde to give the product. In the present study, $NaAlO_2$ is strong base catalyst and showed excellent performance even at room temperature with short reaction time (2 h). Yet, $NaAlO_2$ in its pure solid form is highly hygroscopic and corrosive, and thereby difficult to handle.[28] Hence supporting $NaAlO_2$ on a suitable support was inspected.

Various homogeneous and heterogeneous catalysts are reported for Knoevenagel condensation reactions and the recent results are listed in the Table 3 along with their turnover frequency (TOF), however 20 SA Al_2O_3 results are comparable with reported results and the reactions are conducted in the absence of any solvent at room temperature.

In order to understand the effect of support in generating basicity in mesoporous materials, silica, alumina and titania are selected. The basicity measurement from CO_2-TPD also showed that, 20 $SASiO_2$ total basicity is relatively low; as a result, it showed low activity in the condensation reaction studied.

On the other hand, SA-promoted alumina possess high surface basic strength and showed higher BA conversion. From the results, it is clear that the alumina-base catalyst is the best material. Further optimization and reusability studies conducted with 20 $SAAl_2O_3$.

The effect of reaction period on the conversion of BA was studied from 30 min to 4 h. BA conversion increased with increase in time up to 4 h (Figure S4). The obtained results are also compared with 100% SA being highly basic catalyst it reached maximum conversion within 2 h of reaction time (Figure S4).

To confirm the heterogeneous nature of the catalyst, catalyst filtration test was conducted in solution. The reaction was carried out using 20 $SAAl_2O_3$ and interrupted after 1 h (BA conversion = 65%, far enough from the thermodynamic equilibrium). The reaction mixture containing the catalyst was filtered to remove the solid catalyst. The filtrate was stirred at 30 °C for an additional 3 h in the absence of the catalyst. Analysis of the final reaction mixture showed that, no further BA conversion (Figure 5). This test confirms that, active species (SA) is not leaching during the reaction- the prepared catalysts are heterogeneous. Additionally, Catalysts reusability studies was performed for several cycles of reaction. After each experiment, the catalyst was removed from the reaction mixture by filtration and washed with solvent (5 ml of ethanol, two times) to remove the adsorbed reactants on the surface of the catalyst, and finally it was dried for 4 h at 120 °C. The results presented in Figure 6 indicate that the catalyst can be recycled

Table 2. Catalytic activity of solid base catalysts.

Catalyst	Conversion (%)
Blank	04.0
$NaAlO_2$	96.0
SiO_2	08.0
5SA SiO_2	38.0
10SA SiO_2	51.0
20SA SiO_2	60.0
20SA Al_2O_3	93.0
20SA TiO_2	71.0
Hydrotalcite	15.0
MgO	54.0

Reaction conditions: 5 mmol of BA, 5 mmol of ECA, 0.05 g of catalyst at 30 ^{0}C for 4 h.

Table 3. Comparison of catalytic activity with the reported results.

Catalyst	Conversion (%)	TOF (h^{-1})	References
NAP	94.0	–	[47]
HAP-Cs_2CO_3	75.0	–	[48]
ZnO	87.0	212	[49]
Au/AP-MCF	99.0	269	[50]
20 SA Al_2O_3	93.0	727	Present work
Hydrotalcite	15.0	–	Present work
MgO	54.0	–	Present work

Reaction conditions: Reaction conditions: 5 mmol of BA, 5 mmol of ECA, 50 mg of 20 SA Al_2O_3 catalyst at 30 °C.

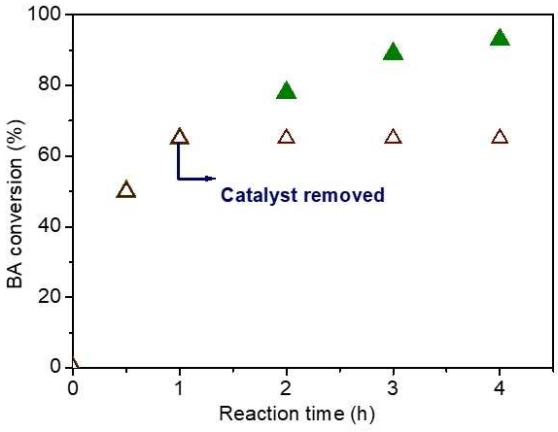

Figure 5. Leaching test with 20 $SAAl_2O_3$ catalyst.

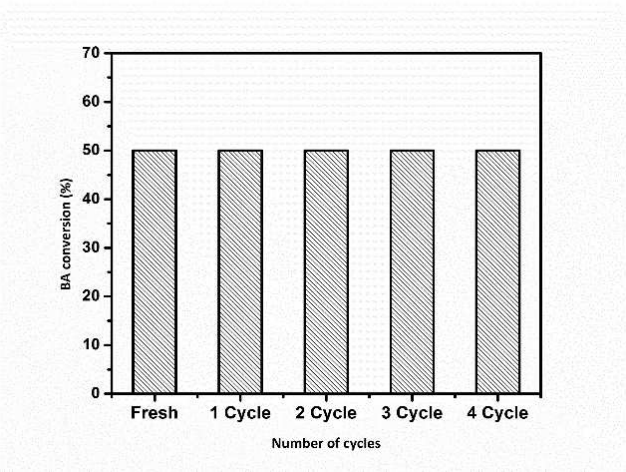

Figure 6. Reusability studies at lower conversion rates. Reaction conditions: 5 m mol of BA, 5 m mol of ECA, 50 mg of catalyst at 30 °C for 30 min.

and reused up to four times with no significant loss in BA conversion. To confirm further, the reusability studies at higher conversion of BA are also studied (Figure S5), from the results it is confirmed that, the catalysts are truly heterogeneous, no loss in activity up to 4 cycles. The spent catalyst was characterized by BET and CO_2-TPD and the no change in basicity or structural changes are observed after 4 cycles (Table S1).

BA conversion as a function of time with 20 SA Al_2O_3 catalyst (Green triangle) and results of the filtration test where the catalyst was removed by filtration after 1 h (Red triangles). Reaction conditions: 5 mmol of BA, 5 mmol of ECA, 50 mg of 20 SA Al_2O_3 catalyst at 30 °C.

3. Conclusions

Novel sodium aluminate based mesoporous solid catalysts was designed by promoting it on mesoporous silica, titania and alumina by one pot preparation method. Sodium aluminate, a basic solid material and is highly active catalyst in non-aqueous solvents for various organic transformations. Indeed, it is corrosive, hygroscopic, which makes it difficult for catalytic applications. Promoting this solid super base on mesoporous solids was shown to be a relevant strategy for catalytic studies. The surface area and pore volume of the mesoporous solids is strongly decreased with sodium aluminate promotion. Overall, the catalysts showed full selectivity and high activity for the condensation of benzaldehyde with ethylcyanoacetate at room temperature under solvent free reaction conditions. They truly act as a heterogeneous catalyst and show excellent reusability and stability. The newly developed solids are highly active basic catalysts for condensation reactions and can be used for other base catalyzed organic transformations.

Supporting Information Summary

All experimental procedures for the catalysts synthesis and techniques used for the characterization are available in the supporting information file.

Acknowledgements

Authors gratefully acknowledge the Walloon Region for the financial support (BEWARE programme, convention n° 1410279) and Dequenne Chimie for providing the sodium aluminate solution.

Keywords: green reaction conditions · Knoevenagel condensation · mesoporous catalysts · sodium aluminate

[1] G. Busca, *Chem. Rev.* **2010**, *110*, 2217–2249.
[2] L. B. Sun, X. Q. Liu, H. C. Zhou, *Chem. Soc. Rev.* **2015**, *44*, 5092–5147.
[3] Y. Ono, *J. Catal.* **2003**, *216*, 406–415
[4] D. P. Debecker, E. M. Gaigneaux, G. Busca, *Chem. Eur. J.* **2009**, *15*, 3920–3935.
[5] S. Baljeet, M. K. R. G. C. S. M. P. K. P. Vivek, *Angew. Chem. Int. Ed.* **2015**, *54*, 5985–5989; *Angew. Chem.* **2015**, *127*, 6083–6087.
[6] H. Hattori, *Appl. Catal. A* **2015**, *504*, 103–109.
[7] H. Hattori, *Appl. Catal. A* **2001**, *222*, 247–259.
[8] R. Radhakrishan, D. M. Do, S. Jaenicke, Y. Sasson, G. K. Chuah, *ACS Catal.* **2011**, *1*, 1631–1636.
[9] R. Xing, H. Wu, X. Li, Z. Zhao, Y Liu, L. Chen, P. Wu, *J. Mater. Chem.* **2009**, *19*, 4004–4011.
[10] A. D. Murkute, J. E. Jackson, D. J. Miller, *J. Catal.* **2011**, *278*, 189–199.
[11] N. Kumar, E. Leino, P. Mäki-Arvela, A. Aho, M. Käldström, M. Tuominen, P. Laukkanen, K. Eränen, J.-P. Mikkola, T. Salmi, D. Y. Murzin, *Microporous Mesoporous Mater.* **2012**, *152*, 71–77.
[12] R. B. LaPierre, A. C. Rohrman Jr, J. L. Schlenker, J. D. Wood, M. K. Rubin, W. J. Rohrbaugh, *Zeolites* **1985**, *5*, 346–348.
[13] R. P. Dimitrov, B. Anissa, D. Jean-Pierre, M. Alexandre, D Véronique, *Adv. Synth. Catal.* **2011**, *353*, 2067–2077
[14] D. P. Debecker, *Chem. Rec.* **2018**, *18*, 662–675.
[15] X.-Y. Liu, L.-B. Sun, X.-D. Liu, A.-G. Li, F. Lu, X.-Q. Liu, *ACS Appl. Mater. Interfaces* **2013**, *5*, 9823–9829.
[16] J. A. Melero, R. van Grieken, G. Morales, *Chem. Rev.* **2006**, *106*, 3790–3812.
[17] T. Yokoi, Y. Kubota, T. Tasumi, *Appl. Catal. A* **2012**, *422*, 14-37.
[18] J. M. Lopez Pestana, M. J. Avila Rey, R. M. Martin Aranda, *Green Chem.* **2002**, *4*, 628–630.
[19] S. Ramesh, D. P. Debecker, *Catal. Commun.* **2017**, *97*, 102–105.
[20] V. Mutreja, S. Singh, A. Ali, *J. Oleo Sci.* **2012**, *61*, 665–669.
[21] S. K. Cherikkallinmel, A. Gopalakrishnan, Z. Yaakob, R. M. Ramakrishnan, S. Sugunan, B. N. Narayanan, *RSC Adv.* **2015**, *5*, 46290–46294.
[22] R. Bai, P. Liu, J. Yang, C. Liu, Y. Gu, *ACS Sustainable Chem. Eng.* **2015**, *3*, 1292–1297.
[23] S. Lou, L. Jia, X. Guo, W. Wu, L. Gao, H. Wu, J. Wang, *RSC Adv.* **2016**, *6*, 6921–6931.
[24] T. Wan, P. Yu, S. Wang, Y. Luo, *Energy Fuels* **2009**, *23*, 1089–1092.
[25] W. Li, S. Ramesh, J. Estager, J. C. M. Monbaliu, D. P. Debecker, P. Luis, *Chem. Eng. Process.* **2018**, *132*, 127–136.
[26] S. Ramesh, K. Indukuri, O. Riant, D. P. Debecker, *Org. Process Res. Dev.* **2018**, *22*, 1846–1851.
[27] A. V. Agafonov, I. A. Yamanovskaya, V. K. Ivanov, G. A. Seisenbaeva, V. G. Kessler, *J. Sol-Gel Sci. Technol.* **2015**, *76*, 90–97.
[28] S. Ramesh, D. François, V. D. B. Ludivine, D. P. Debecker, *ChemCatChem* **2018**, *10*, 1398–1405.
[29] Y. Ning, S. Niu, S. Zhao, X. Zhang, Y. Zhang, K. Han, C. Lu, X. Zhang, *ChemistrySelect* **2019**, *4*, 9849–9856.
[30] Y. Zhang, S. Niu, C. Lu, Z. Gong, X. Hu, *Energy Convers. Manage.* **2019**, 203, 112263–112274.

[31] S. Ramesh, D. François, D. P. Debecker, *Appl. Catal. A* **2019**, *581*, 31-36.
[32] K. S. W. Sing, D. H. Everett, R. A. W. Haul, L. Moscou, R. A. Pierotti, J. Rouquerol, T. Siemienewska, *Pure Appl. Chem.* **1985**, 603–619.
[33] A. Kim, D. P. Debecker, F. Devred, V. Dubois, C. Sanchez, C. Sassoye, *Appl. Catal. B* **2018**, *220*, 615-625.
[34] K. Sakurai, M. Mizusawa , *Anal. Chem.* **2010**, *82*, 3519–3522.
[35] Y. Wang, K. Shih, X. Jiang, *Ceram. Int.* **2012**, *38*, 1879–1886.
[36] H. Kleineberg, M. Eisenacher, H. Lange, H. Strutz, R. Palkovits, *Catal. Sci. Technol.* **2016**, *6*, 6057–6065.
[37] D. Cornu, H. Guesmi, G. Laugel, J. Marc Kraft, H. L. Pernot, *Phys. Chem. Chem. Phys.* **2015**, *17*, 14168–14176.
[38] L. B. Sun, F. N. Gu, Y. Chun, J. Yang, Y. Wang, J. H. Zhu, *J. Phys. Chem. C* **2008**, *112*, 4978–4985.
[39] W. C. Wilfong, C. S. Srikanth, S. S. C. Chuang, *ACS Appl. Mater. Interfaces* **2014**, *6*, 13617–13626.
[40] D. Cornu, H. Guesmi, J. M. Krafft, H. Lauron-Pernot , *J. Phys. Chem. C* **2012**, *116*, 6645–6654.
[41] S. Ramesh, B. S. Jai Prakash, Y. S. Bhat, *Curr. Organo catal.* **2015**, *2*, 51–57.
[42] M. Opanasenko, A. Dhakshninamoorthy, M. Shamzhy, P. Nachtigall, M. Horacek, H. Garcia, J. Cejka, *Catal. Sci. Technol.* **2013**, *3*, 500–5007.
[43] B. Viswanadham, P. Jhani, K. V. R. Chary, H. B. Friedrich, S. Singh, *Catal. Lett.* **2016**, *146*, 364–372.
[44] N. Shcherban, P. Maki-Arvela, A. Aho, S. Sergiienko, P. Yaremov, K. Eranen, D. Murzin, *Catal. Sci. Technol.* **2018**, 8, 2928–2937.
[45] E. V. Dalessandro, H. P. Collin, M. S. Valle, J. R. Pliego, *RSC Adv.* **2016**, *6*, 57803–57810.
[46] B. Sakthivel, A. Dhakshinamoorthy, *J. Colloid Interface Sci.* **2017**, *485*, 75–80.
[47] K. Isobe, T. Hoshi, T. Suzuki, H. J. M. D. Hagiwara, *Mol.* **2005**, *9*, 317–320.
[48] M. Gupta, R. Gupta, M. Anand, *Beilstein J. Org. Chem.* **2009**, *5*, 68–74.
[49] Li, A. A. Adesina, E. M. Kennedy, M. Stockenhuber, *Phys. Chem. Chem. Phys.* **2017**, *19*, 26630–26644.
[50] I. Sobczak, V. Calvino-Casilda, L. Wolski, T. Siodla, R. Martin Aranda, M. Ziolek, *Catal. Today* **2019**, *325*, 81–88.

Submitted: October 29, 2019
Accepted: December 17, 2019